

RESEARCH ARTICLE

Radiation-Induced 3D Genome Structure Reorganization Regulates Gene Transcription

Zhihong Zhang[†], Yazhi Xiao[†], Xinrong He, Yiyao Chen, Hailong Sheng, Zhenru Zhu, Jingyuan Sun^{*}, Chuanhui Cao^{*}

Department of Radiation Oncology, Nanfang Hospital, Southern Medical University, Guangzhou, 510515, China

[†]These authors contributed equally to this work.

Received: October 22, 2022
Accepted: December 9, 2022
Published Online: January 16, 2023

***CORRESPONDING AUTHORS**

Dr. Chuanhui Cao
E-mail: huichuancao@163.com
Dr. Jingyuan Sun
E-mail: 15013050515@163.com

CITATION

Zhang Z, Xiao Y, He X, *et al.*, 2022, Radiation-Induced 3D Genome Structure Reorganization Regulates Gene Transcription. *Cancer Plus*, 4(2):37-46.
DOI: [10.18063/cp.v4i2.391](https://doi.org/10.18063/cp.v4i2.391)

Copyright: © 2023

Zhang, *et al.* This is an Open Access article distributed under the terms of the Creative Commons Attribution-NonCommercial 4.0 International License (<http://creativecommons.org/licenses/by-nc/4.0/>), permitting all noncommercial use, distribution, and reproduction in any medium, provided the original work is properly cited.

Abstract: Radiation can induce cellular three-dimensional (3D) genome reorganization. However, the exact functional relevance of spatial rearrangements to gene transcription remains unknown. First, we screened and profiled the global picture of the 3D genome structure reorganization in human hepatocellular carcinoma cells MHCC-LM3 that were irradiated with 4Gy X-ray at a concentration of 100 cGy/min for 4 min using the high-throughput chromosome conformation capture (Hi-C) technique. They were mapped and analyzed at three levels: compartment, topologically associating domain (TAD) and TAD boundary, and loop. The regulatory relationships within gene transcription exerted by the related dynamic spatial structure were confirmed by ribonucleic acid sequencing (RNA-seq) and further experimentally confirmed by quantitative real-time polymerase chain reaction in the same treated cell samples. A significant increase in interchromosomal interactions was observed in the irradiated cells. The extent of the effect of dynamic compartment switches and disrupted and gained TAD boundaries on gene transcription was significantly greater than that of small differential chromatin loops. Genes in human leukocyte antigen (*HLA*) and C-C motif chemokine ligand (*CCL*) gene clusters associated with TAD boundary alterations were considerably upregulated, and this effect was maintained 24 h post-radiation. We characterized the radiation-induced landscape map of the 3D genome in cells and elucidated the mechanism by which 3D genome reorganization spatially regulates gene transcription. This study provides a basis for further research directed toward understanding the role of structural alterations in gene expression.

Keywords: Carcinoma cells; X-ray; Three-dimensional genomes; Rearrangement; Gene transcription regulation

1. Introduction

Up to 50% of cancer patients are treated with radiotherapy, which is an indispensable technique to fight against cancers^[1]. Radiation can eliminate cancer cells based on (i) cytotoxicity from direct deoxyribonucleic acid (DNA) damage and (ii) reprogramming of the tumour immunity microenvironment into an immunostimulatory one, which is closely related to gene expression profiles^[2]. Gene expression can be regulated genetically or epigenetically through single nucleotide variants, indels, DNA hydroxymethylation, N⁶-methyladenosine, and micro-ribonucleic acid (miRNA)^[3-6]. Expression units are assembled by spatial clustering of local genes and distant regulatory elements, which provide extra gene regulation through the combinatorial association of genes and sets of regulatory

elements^[7]. Since the DNA helix hierarchically organizes into higher-order structures, the spatial arrangement of the genome dramatically affects multiple DNA functions^[8]. Understanding the role of radiation-induced cellular genome reorganization in gene expression regulation requires more than just knowledge of the linear genome.

Our understanding of the role of dynamic 3D structures is substantially expanding as a result of the rapidly developing chromosome conformation capture techniques^[9]. High-throughput chromosome conformation capture (Hi-C) has revealed that a genome is folded into a gene-dense transcriptionally active compartment A and transcriptionally inactive compartment B^[9]. Topologically associated domains (TADs), as functional units, regulate gene expression and DNA replication^[10,11]. DNA loops within TADs facilitate interactions between remote enhancers and local promoters^[12]. The dynamics of higher-order 3D genome may contribute to gene expression regulation.

Radiation can exert significant effects on 3D genomes that interplay among local chromatin structures, TAD strength, and DNA damage repair^[13]. Several A/B switches have been observed in 5Gy X-ray irradiated fibroblasts and lymphoblasts^[13]. The observed phenomenon of increased TAD boundary strength might be caused by the recruitment of structural proteins, such as CCCTC-binding factor (CTCF) and cohesin, to chromatin, which increases the strength of TAD boundary and decreases the contact frequency across TAD boundaries^[13]. Eventually, it reduces the frequency of deleterious translocation events and maintains genome integrity, thus promoting cell survival following irradiation^[13-16]. Larger structures are more stable, whereas dedicated structures are more variable following irradiation^[17]. The role of radiation-induced dynamics of the 3D genome in regulating gene expression remains unknown thus far.

In this study, we demonstrated that after exposure to radiation, dynamic TAD boundaries-related non-genetic structural regulation occurs in liver cancer cells, elevating the expression of major histocompatibility complex (MHC) molecules and C-C motif chemokine ligand (CCL) chemokines, which may be closely related to antigen presentation and cytotoxic cell recruitment to irradiated sites of cancers, suggesting a promising intervention in the radiotherapeutic process. More research and evidence are needed to translate these finding into cancer treatment in the near future.

2. Materials and methods

2.1. Cell culture

Human hepatocellular carcinoma cell line MHCC-LM3 was obtained from Shanghai Institute of Biochemistry and Cell Biology. Proliferating MHCC-LM3 cells were cultured in Dulbecco's Modified Eagle's Medium (Gibco, USA), supplemented with 10% fetal bovine serum (Gibco) at 37°C in an atmosphere of 5% carbon dioxide (CO₂).

2.2. Radiation treatment

4.00E + 06 LM3 cells in a 10-cm dish (Wuxi NEST, China) were irradiated with X-rays at a dose of 4 Gy using the Varian 23EX Linac Biological Irradiator (Varian, USA). X-rays were emitted at a concentration of 100 cGy/min for 4 min. The cells were, then, cultured under the aforementioned conditions for 30 min. At 30 min after irradiation, the cells were collected and fixed for downstream applications.

2.3. *In situ* high-throughput chromosome conformation capture library preparation

In the preparation of the Hi-C library, *in situ* Hi-C experiments were conducted at appropriate time points according to the protocol described by Lieberman-Aiden *et al.*^[9] and Belton *et al.*^[18]. Briefly, 2.00E + 07 cells were crosslinked with 1% formaldehyde at 25°C for 15 min, quenched with 125 mM glycine for 5 min, and washed with ice-cold phosphate-buffered saline (PBS) containing protease inhibitors. The cells were pelleted (1,000 × g, 5 min at 4°C), and the pellets were then suspended in a cell lysis buffer for permeabilization and homogenized by douncing. DNA was digested overnight at 37°C by adding 400 units DpnII (NEB) to produce sticky ends on both sides of the crosslink. Biotin-labeled bases were introduced to facilitate subsequent DNA purification and capture. DNA was repaired, and cyclization of DNA fragments containing interactions was performed. Biotin-labeled deoxycytidine triphosphates (dCTPs) with unligated ends were removed, and the purified DNA was sheared into 300 bp – 700 bp fragments. Streptavidin magnetic beads were used to capture DNA fragments harboring interactions, and the library was, then, sequenced (Biomarker Technologies, Beijing, China).

2.4. High-throughput chromosome conformation capture data processing

Raw sequence reads in FASTQ format were processed using in-house Perl scripts^[9]. Reads containing adapter sequences, poly-N, and low-quality reads were removed from the raw data. Meanwhile, the Q20, Q30, and guanine-cytosine contents of the clean data were calculated. The two-terminal sequencing data were then aligned with the reference genome or the assembled genome to obtain the neat and only reads using Burrows-Wheeler Aligner^[19]. The reads obtained were analyzed using HiC-Pro v2.10.0^[20] to identify valid and invalid interaction pairs, and the corresponding standardized interaction matrix was obtained. Subsequently, the Pearson correlation coefficient between each biological repeat was calculated. More details are available in the supplemental materials and methods.

2.5. Real-time polymerase chain reaction (RT-PCR)

Total RNA was isolated from non-irradiated and irradiated LM3 cells from the radiation treatment assay using TRIzol®

Reagent (Invitrogen) according to the manufacturer's instructions. Real-time (RT)-PCR was performed using an SYBR Green PCR Kit that was purchased from Takara Biotechnology (Takara, Dalian, China) in Roche Light Cycler® 480. The primers are listed in **Table S1**, and glyceraldehyde 3-phosphate dehydrogenase gene (*GAPDH*) was used as the housekeeping gene for analysis.

$Ct = Ct(\text{target gene}) - Ct(\text{housekeeping gene})$

$Ct = Ct(\text{treatment group}) - Ct(\text{control group})$

$\text{Relative mRNA level} = 2^{-Ct}$

2.6. Statistical analysis

All data in the quantitative (q) RT-PCR experiments were presented as mean \pm standard deviation from three independent experiments. Student's *t*-test was performed to compare the differences between non-irradiated (BLK group) and irradiated cells (IR group). Comparisons between paired data were performed using the Wilcoxon matched-pairs signed-rank test. The difference between the proportion of differential loop-related differentially expressed genes (DEGs) in all DEGs and that of loop-related genes in the whole genome background was determined by Chi-square test (Fisher's exact test). Analysis of correlation was determined by Pearson correlation test. For all statistical analyses, $P < 0.05$ was determined to be significant. Graphs were plotted using GraphPad Prism 9.

3. Results

3.1. Irradiated cells exhibit some alterations in the genome structure

Proliferating human hepatocellular carcinoma cells MHCC-LM3 were irradiated with X-ray at a dose of 4 Gy and analyzed after 30 min (**Figure 1A**). Hi-C libraries of non-irradiated cells (BLK group) and irradiated cells (IR group) were constructed and sequenced (**Table S2**). Interactions were visualized in chromosome heatmaps of BLK and IR cells (**Figure 1B**). The log ratio of contact frequency showed only minor intrachromosomal interaction changes, but an increase in interchromosomal contact in IR cells (**Figure 1B**). Consistently, the probability of interchromosomal contact among pairs of chromosomes showed that small and gene-rich chromosomes (chr 16, 17, 19, 20, 21, and 22) interacted with each other more frequently than larger chromosomes (**Figure 1C**). Similarly, we found a significant negative correlation between trans-contact probability and relative chromosome length (Pearson's $r = -0.5466$ and $P = 0.0070$) (**Figure 1D**). Collectively, these results indicated that the whole-genome differences between BLK and IR cells were relatively small.

3.2. Characterization of genome reorganization at different scales in response to irradiation

The high-resolution contact map was examined after observing the interaction alterations in genome-wide

contact heatmaps. Individual chromosome contact map showed subtle changes between IR and BLK cells (**Figure 2A**). However, only a few compartment identity switches (~2%) in IR cells were observed in the whole genome (**Figure 2B**). Intriguingly, the genes that had switched from B to active A compartments were enriched in gene ontology (GO) terms of radiation-related functional categories, such as double-strand break repair (GO: 0000724, $P = 0.0014$, enrichment factor = 4.09) and DNA damage checkpoint (GO: 0000077, $P = 0.0081$, enrichment factor = 4.88) (**Table S3**).

TADs are formed at a sub-megabase scale as functional units for regulating gene expression and DNA replication. The two basic features of TADs include self-association of regions within TADs and insulation between neighboring TADs^[21]. Although the number of lost TAD boundaries was greater than that of gained boundaries in each chromosome (**Figure 2C**), there was no significant increase in the number of TADs, and the irradiated cells had a larger TAD size (0.65 Mb in BLK cells versus 0.67 Mb in IR cells, $P < 0.0001$) (**Figure 2D**). Only 245 BLK-specific TAD boundaries (4.49%) and 122 radiation-specific TAD boundaries (2.25%) were identified (**Figure 2E**). RNA-seq data revealed that the proportions of downregulated and upregulated genes out of the genes associated with gained or disrupted TAD boundaries shared almost the same percentage, that is, 36.68% in disrupted BLK-specific boundaries and 37.57% in gained radiation-specific boundaries of downregulated genes as compared to 39.32% in the whole genome; 29.04% and 27.32% of upregulated genes in BLK and IR cells, respectively, as compared to 26.83% in the background genes (**Figure 2F**). These DEGs were also enriched in several Kyoto Encyclopedia of Genes and Genomes (KEGG) pathways, including antigen processing and presentation (KO04612, $P = 0.0014$, enrichment factor = 3.06) and chemokine signalling pathway (KO04062, $P = 0.08$, enrichment factor = 1.53) (**Table S4**).

Following that, we identified differential chromatin loops to investigate the promoter interactions that contribute to gene transcription (**Figure 3A**). A total of 119 out of 18,444 loops and 113 out of 17,668 loops were identified as lost and gained loops with high confidence in BLK and IR cells, respectively (**Figure 3B**). More than half of these loops were identified as enhancer-promoter loops, including one enhancer-promoter loop, two enhancer-promoter loop, and three and over three (three+) enhancer-promoter loop (12,180 or 65.78% in BLK cells and 11,800 or 66.4% in IR cells) (**Figure 3C**). Among all DEGs, the proportion of DEGs anchored by differential loops was higher than that of all DEGs related to dynamic loops in the whole genome (Chi-squared test, $P < 0.05$) (**Figure 3D**), indicating that radiation-induced differential loops have a more significant regulatory effect on gene expression than those without exposure to radiation.

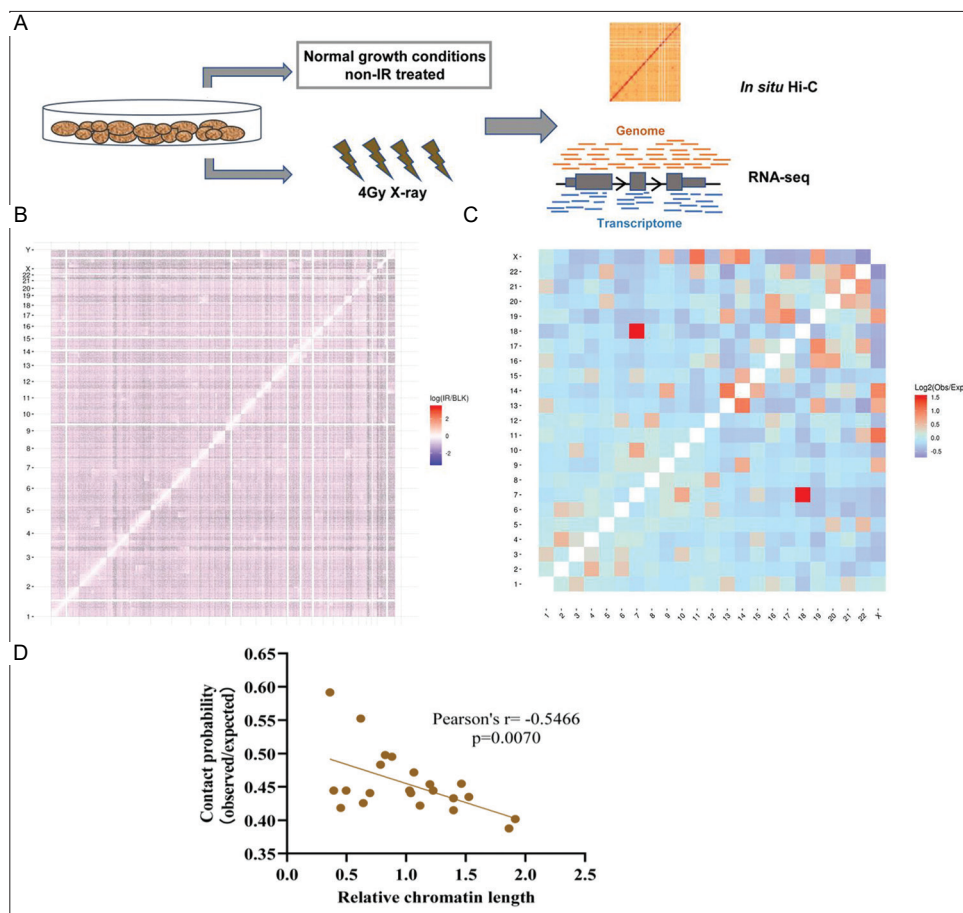


Figure 1. Cancer cells exhibit subtle changes in genome structure after irradiation. (A) Schematic diagram of datasets generated and analyzed in this study. Human cancer cells with or without exposure to 4Gy X-ray were used to generate *in situ* high-throughput chromosome conformation capture datasets and their corresponding ribonucleic acid sequencing (RNA-seq) data. (B) $\log_2(\text{IR/BLK})$ contact map in 0.5 Mb bins. (C) Observed/expected number of contacts between any pairs of 23 chromosomes. Red indicates enrichment, while blue indicates depletion. (D) Observed/expected interactions plotted against the relative chromosome length. The line represents the linear trend for obtained values.

3.3. The extent of transcriptional regulation by radiation-induced dynamic genome reorganization differs among altered spatial structures

To explore the extent of the regulatory effect of different radiation-induced dynamic genome structures on transcription, the same batch of cells in Hi-C experiment was subjected to RNA-seq (Table S2). We examined and compared the transcription levels in altered spatial structures and found that genes were upregulated by 8.59% or downregulated by 9.17% in altered compartments, upregulated by 9.99% or downregulated by 10.63% in altered TAD boundaries, and upregulated by 5.49% or downregulated by 3.49% in dynamic DNA loops (Figure 4A). Interestingly, the same level of regulation was observed for dynamic compartments with an “A to B” or “B to A” switch for gained or lost loops (upregulated or downregulated by ~9% or ~5% in compartments and DNA loops, respectively) (Figure 4B). Intriguingly,

the percentage of transcriptionally regulated genes in disrupted TAD boundaries (upregulated by 12.79%, or downregulated by 15.53%) was significantly higher than that of those in newly formed boundaries (upregulated by 7.68%, or downregulated by 7.76%) (Figure 4B). Together, these results suggest that TAD boundary disruption may exert more transcriptional control on gene activity.

3.4. Radiation-induced alteration of TAD boundaries promotes the transcription of radiation-related gene clusters

Extensive chromosomal reorganization often disrupts boundaries, thus inducing the merging of neighbouring TADs^[22]. Therefore, genes that were previously widely spaced can enter each other's contact search space and form a new regulatory circuit (Figure 5A)^[23]. Experimental deletion of TAD boundaries has indicated that the merging of TADs induces regulatory rewiring and alters gene transcription^[22,24-26]. Within the region of disrupted TAD

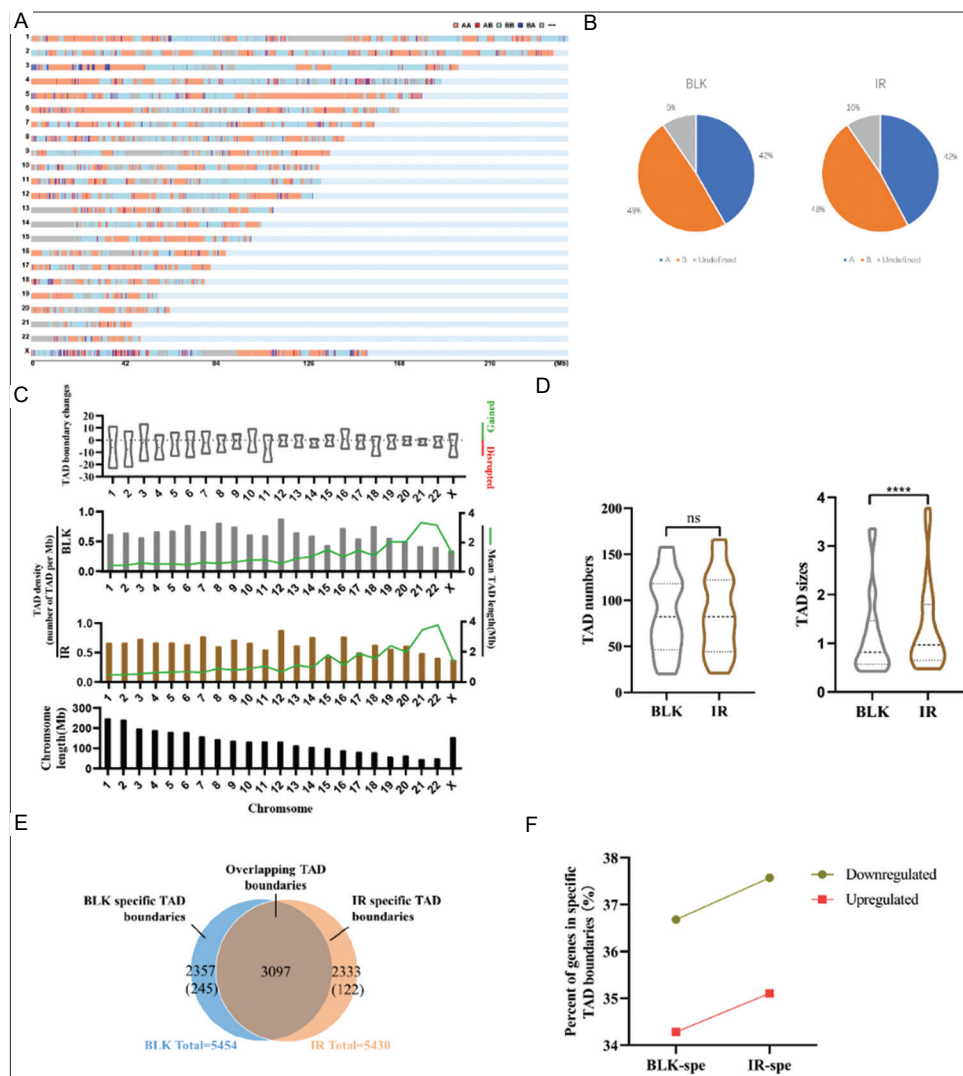


Figure 2. Characterization of genome reorganization at compartments and topologically associated domains (TADs) after irradiation. (A) Genome-wide map of compartment identity switches. The chromosome regions and compartment identity switches, including static compartments (AA or BB) or dynamic compartments (AB or BA) in each chromosome, are shown. (B) Pie charts showing the proportion of static and dynamic compartments in BLK and IR cells. “A” and “B” denote open and closed compartments, respectively; “AA” represents compartments that are open in both cell line, while “BB” represents compartments that are closed in both cell lines; “AB” denotes compartments that are open in BLK cells but closed in IR cells, while “BA” denotes compartments that are closed in BLK cells but open in IR cells. (C) Relative chromosome length (bottom). TAD density, and mean TAD length in each chromosome (middle). Numbers of TAD boundaries lost or gained in each chromosome (top); positive and negative values represent the numbers of TAD boundaries gained and lost, respectively. (D) Violin plot indicating the number and average size (in Mb) of TADs identified in both BLK and IR cells. (E) Venn diagram showing that over half of all TAD boundaries between BLK and IR cells were conserved. (F) Proportion of downregulated and upregulated genes (%) located in specific lost or gained TAD boundaries.

boundaries, we found that both the *HLA* gene cluster on chr6 (*p21.32*) and the *CCL*-associated gene cluster on chr17 (*q12*) (Figure 5B–E) were closely related to the irradiation response^[27,28] (Table S4). RNA-seq data showed significant transcriptional changes in these associated genes 30 min after irradiation, except for *HLA-DMA*. The expression levels of *HLA-DMA*, *HLA-DMB*, *HLA-DRA*, and *HLA-DPB1* genes were found to be significantly higher than those of genes located in the original boundaries (Figure 5C). Moreover, we observed an increase in the expression levels of *CCL1*,

CCL13, and *CCL3L1* (Figure 5E). In contrast, no apparent increase in the expressions of *HLA-DMA* and *CCL13* was observed 30 min after irradiation (Figures 5C and 5E). In addition, the increase in gene expression induced by disrupted TAD boundaries was maintained 24 h after irradiation (Figures 5C and 5E). In short, the disruption of TAD boundaries (or the merging of TADs) may exert a substantial level of regulatory control on gene transcription in response to radiation.

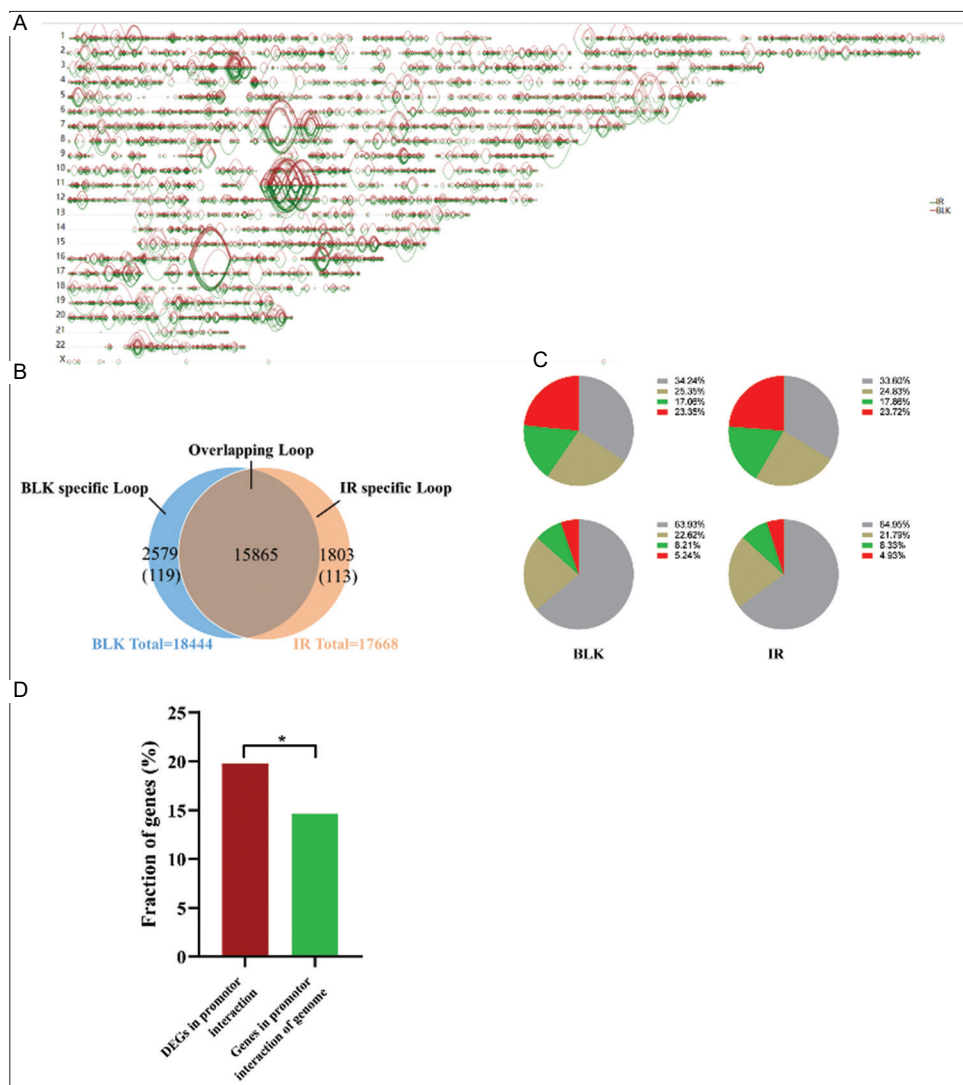


Figure 3. Genes related to chromatin loops were enriched differentially expressed genes (DEGs). (A) Genome-wide map of differential chromatin loops. The loop anchored sites, the connection of the two loci, and the interaction strength (the height of the parabola) are shown. (B) Venn diagram showing that the majority (~89%) of the chromatin loops between BLK and IR cells were conserved. (C) Pie charts showing the proportion of both promoter loops (top: no promoter loop, one-promotor loop, two-promotor loop, and three⁺-promotor loop) and enhancer-promotor loops (bottom: no enhancer loop, one enhancer-promotor loop, two enhancer-promotor loop, and three⁺ enhancer-promotor loop). (D) Histogram showing that genes related to BLK- or IR-specific chromatin loop genes were significantly enriched in DEGs in the RNA sequencing data after irradiation compared with those in the genome background.

4. Discussion

Dynamic 3D genome plays a role in various cellular biological processes, including cancer initiation and development. The role of radiation-induced dynamic spatial genome reorganization in transcription regulation remains unknown thus far. By understanding the role of 3D genome in the observable radiotherapeutic effect, radiation application would be more controllable and efficient. Here, we characterized the changes in the 3D genome of a type of cancer cell following exposure to radiation. First, a small effect of irradiation was observed on A/B compartment switching, and genes switching from B to A compartments were enriched in GO terms of radiation-related functional

categories (Tables S3 and S5). Second, irradiated cells had a larger TAD size and an increased number of disrupted TAD boundaries. Third, we found increased proportions of DEGs anchored by differential chromatin loops on irradiation. In addition, genes in the *HLA* cluster on chr6 (p21.32) and *CCL* cluster on chr17 (q12) within the region of disrupted TAD boundary in IR cells were subjected to more regulation from 3D genome dynamics. These findings suggest that the TAD state may regulate gene expression the most in response to irradiation. Our findings provide novel insights into the roles of radiation-induced reorganization in the spatial control of gene transcription.

Cells are frequently exposed to different stresses, including thermal, osmotic, and hypoxic signals, as well

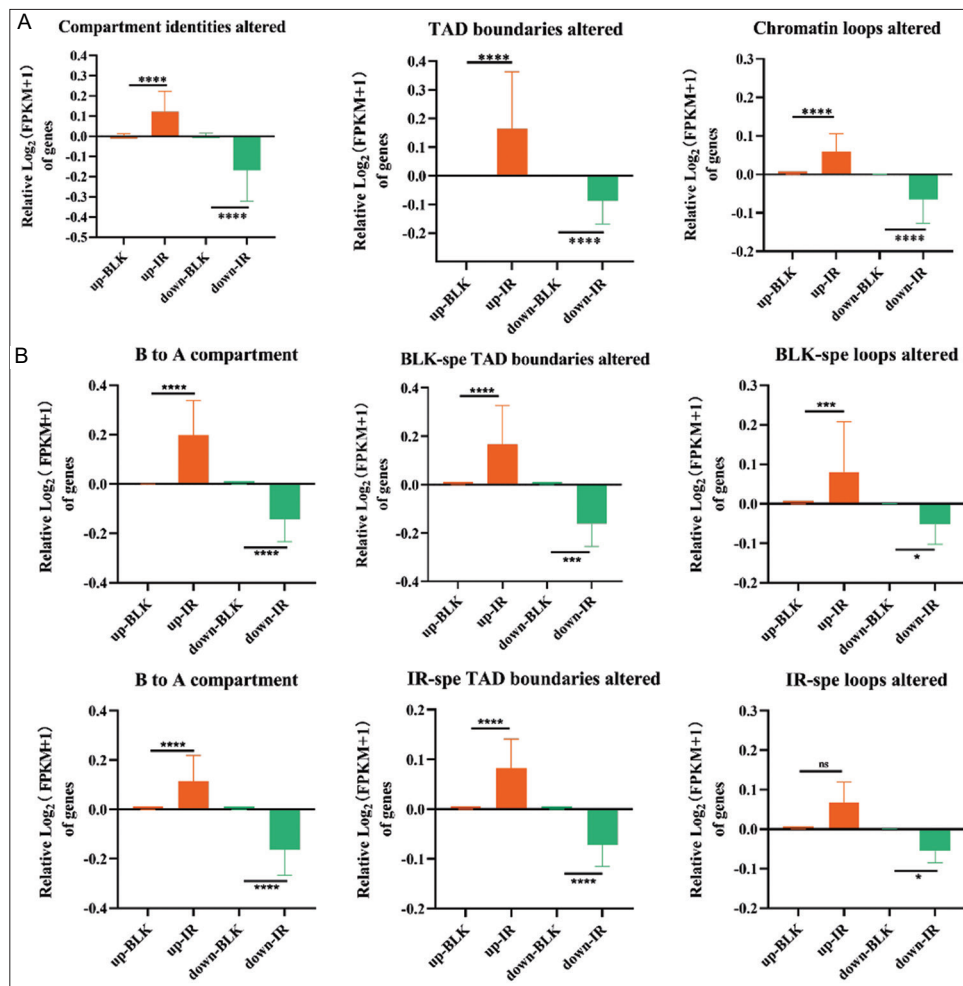


Figure 4. Regulatory potential of radiation-induced alteration of compartment, topologically associating domain (TAD) boundaries, and chromatin loops in transcription. Quantitation of gene expression changes, grouped by radiation-induced alteration of compartment, TADs, and chromatin loops, in (A) all different genes or (B) those of BLK-specific or IR-specific structures. Student's t-test, * $P < 0.05$, ** $P < 0.01$, *** $P < 0.001$, **** $P < 0.0001$.

as other internal signals from differentiation, development, or replicative senescence^[29,30]. The global chromatin architecture seems to be preserved on exposure to radiation. In contrast, a variety of contact changes have been observed in lymphoblastoid cells 30 min after exposure to 5 Gy X-ray^[13]. The discrepancy in findings may be explained by the difference in radiation dose and specific cell types. Structurally, only a few dynamic genome compartments were identified; this is consistent with the observations of compartment identity switches ($< 1\%$) in BJ-5ta and GM12878 cells that were subjected to 5 Gy X-ray irradiation^[13]. Interestingly, we found significantly larger TADs in IR cells but no difference in the number of TADs. A considerable number of disrupted boundaries was found in IR cells, which was approximately twice that of newly gained boundaries. Moreover, TAD identification based on different algorithms, data input, and data depth, especially resolution, leads to a variability in number, size distribution, and nesting^[17].

At the functional level, the gene expression levels in both clusters were significantly upregulated and maintained for 24 h. At the structural level, no switches of compartment identity in *HLA* genes, *CCL1*, and *CCL13* were observed; however, *CCL3L1* underwent a switch from B to A. Sanders *et al.* have reported that radiation will not affect the interaction strength within compartments due to the variation that exists in globally weak compartment strengths among experimental replicates^[13]. Chromatin loops anchored in promoters or enhancers are basic spatial structures that regulate gene expression. Furthermore, we identified several vital promoter interactions following exposure to radiation. These interactions were found to be associated with dynamic gene expression as the library resolution did not cover a single gene due to the limitations of the currently available techniques. Further studies on promoter interactions, primarily promoter-enhancer interactions, at a higher resolution might provide more accurate and precise information about the spatial regulatory mechanisms of

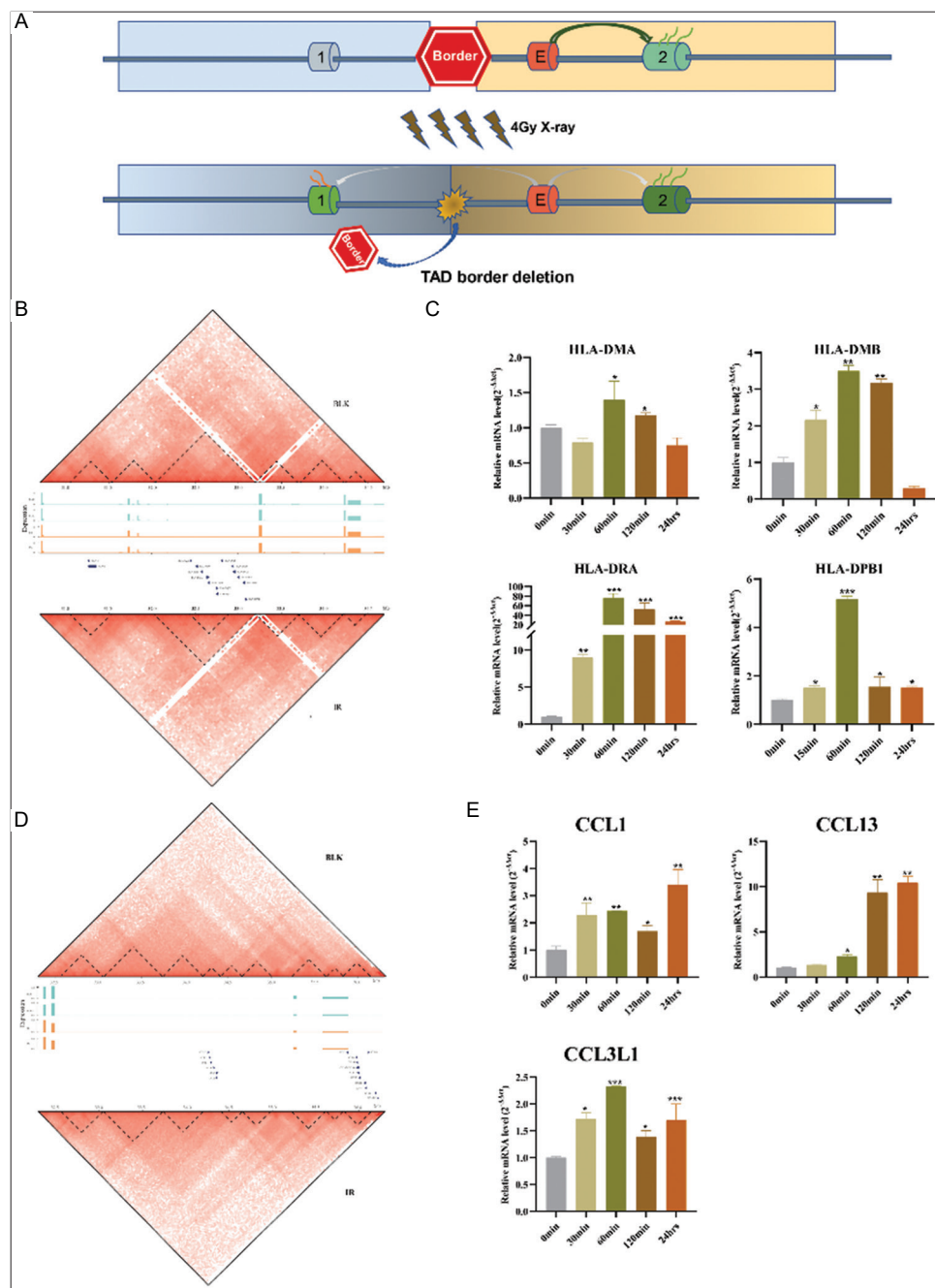


Figure 5. Radiation-induced alteration of topologically associating domain (TAD) boundaries increases radiation-related gene cluster activity. (A) Hypothetical locus with two neighboring TADs (blue and yellow shading), two genes (1 and 2), and one enhancer (E). The disruption of TAD boundaries following exposure to radiation can result in the merging of TADs. Gene 1 is no longer insulated, and thus activated by enhancer E in the previously insulating neighboring TAD. (B) and (D) Contact heatmaps of radiation-related *HLA* gene cluster, (B) including *HLA-DMA*, *HLA-DMB*, *HLA-DRA*, and *HLA-DPB1*, which are located on chr 6: 33075790–32445046, and *CCL* gene cluster, and (D) including *CCL1*, *CCL13*, and *CCL3L1*, which are located on chr17: 34356480–36196758. The plotted locus is from 2 Mb upstream to 2 Mb downstream region. RNA sequencing data and RefSeq gene tracks are shown below the Hi-C heatmaps. (C) and (E) Expression of genes located in the two gene clusters mentioned in (B) and (D). Student's t-test, * $P < 0.05$, ** $P < 0.001$, and *** $P < 0.0001$.

gene transcription. Together, our findings showed that the expression of gene clusters is mainly regulated by the TAD state, partly through compartment identity switching or the formation of new enhancer-promoter chromatin loops.

The effect of radiotherapeutic outcome primarily occurs through direct DNA damage or an indirect cytotoxic effect with the aid of the immune system. Radiation promotes the release of tumor neoantigens and enhance their detectability

through the upregulation of MHC molecule expression or by priming the immunosuppressive tumour immunity microenvironment, leading to increased intratumoral infiltration of cytotoxic CD8⁺ T-cells through chemokine recruitment. We identified that radiation-related genes in two critical clusters on chr6 and chr17 might be regulated by dynamic spatial structures, especially disrupted TAD boundaries, which are closely related to MHC molecule and CD8⁺ T-cell recruitment. Our findings shed light on the mechanism through which radiation may contribute to the priming of the tumour immunity microenvironment through spatial genome reorganization.

5. Conclusion

In this study, we identified numerous dynamic chromatin interactions in response to irradiation at various spatial levels. Our findings demonstrated that dynamic spatial genome reorganization at specific levels is likely to be involved in transcription regulation. This study lays the groundwork for further research on radiation-induced transcription regulation, which will, further, contribute to the understanding of the role of radiation-induced genome alterations. Further research on these 3D structures and higher resolution assays may help us delve deeper into the dynamics of chromatin architecture and the interactions induced by radiation.

Acknowledgments

None.

Funding

We acknowledge support of the National Nature Science Foundation of China (81903133, 82073343), Chinese Postdoctoral Science Foundation (2020M672736), Natural Science Foundation of Guangdong Province (2021A1515012151), and Guangzhou Technology Project (201906010087).

Conflict of interest

The authors declare that they have no competing interests.

Author contributions

Data curation: Zhihong Zhang, Xinrong He, Yiyao Chen, Hailong Sheng and Zhenru Zhu; Formal analysis: Zhihong Zhang, Yazhi Xiao and Yiyao Chen; Funding acquisition: Huichuan Cao; Investigation, Huichuan Cao; Resources: Zhihong Zhang and Yazhi Xiao; Software: Zhihong Zhang, Xinrong He and Hailong Sheng; Supervision: Jingyuan Sun and Huichuan Cao; Validation: Zhenru Zhu; Writing – original draft: Zhihong Zhang and Yazhi Xiao; and Writing – review and editing: Jingyuan Sun and Huichuan Cao.

Ethics approval and consent to participate

Not applicable.

Availability of data

All relevant data are available from within the article and its Supplementary File or can be obtained from the corresponding author on reasonable request.

References

1. Begg AC, Stewart FA, Vens C, 2011, Strategies to Improve Radiotherapy with Targeted Drugs. *Nat Rev Cancer*, 11:239–53. DOI: 10.1038/nrc3007
2. Wang Y, Liu ZG, Yuan H, *et al.*, 2019, The Reciprocity between Radiotherapy and Cancer Immunotherapy. *Clin Cancer Res*, 25:1709–17. DOI: 10.1158/1078-0432.Ccr-18-2581
3. Kageyama SI, Du J, Kaneko S, *et al.*, 2021, Identification of the Mutation Signature of the Cancer Genome Caused by Irradiation. *Radiother Oncol*, 155:10–6. DOI: 10.1016/j.radonc.2020.10.020
4. Becker BV, Kaatsch L, Obermair R, *et al.*, 2019, X-ray Irradiation Induces Subtle Changes in the Genome-Wide Distribution of DNA Hydroxymethylation with Opposing Trends in Genic and Intergenic Regions. *Epigenetics*, 14:81–93. DOI: 10.1080/15592294.2019.1568807
5. Xiang Y, Laurent B, Hsu CH, *et al.*, 2017, RNA m(6) A Methylation Regulates the Ultraviolet-Induced DNA Damage Response, *Nature*, 543:573–6. DOI: 10.1038/nature21671
6. Ramakrishnan V, Xu B, Akers J, *et al.*, 2020, Radiation-Induced Extracellular Vesicle (EV) Release of miR-603 Promotes IGF1-Mediated Stem Cell State in Glioblastomas. *EBioMedicine*, 55:102736. DOI: 10.1016/j.ebiom.2020.102736
7. Dekker J, 2008, Gene Regulation in the Third Dimension. *Science*, 319:1793–4. DOI: 10.1126/science.1152850
8. Woodcock CL, 2006, Chromatin Architecture. *Curr Opin Struct Biol*, 16:213–20. DOI: 10.1016/j.sbi.2006.02.005
9. Lieberman-Aiden E, van Berkum NL, Williams L, *et al.*, 2009, Comprehensive Mapping of Long-Range Interactions Reveals Folding Principles of the Human Genome. *Science*, 326:289–93. DOI: 10.1126/science.1181369
10. Dixon JR, Selvaraj S, Yue F, *et al.*, 2012, Topological Domains in Mammalian Genomes Identified by Analysis of Chromatin Interactions. *Nature*, 485:376–80. DOI: 10.1038/nature11082

11. Pope BD, Ryba T, Dileep V, *et al.*, 2014, Topologically Associating Domains are Stable Units of Replication-Timing Regulation. *Nature*, 515:402–5.
DOI: 10.1038/nature13986
12. Rao SS, Huntley MH, Durand NC, *et al.*, 2014, A 3D Map of the Human Genome at Kilobase Resolution Reveals Principles of Chromatin Looping. *Cell*, 159:1665–80.
DOI: 10.1016/j.cell.2014.11.021
13. Sanders JT, Freeman TF, Xu Y, *et al.*, 2020, Radiation-Induced DNA Damage and Repair Effects on 3D Genome Organization. *Nat Commun*, 11:6178.
DOI: 10.1038/s41467-020-20047-w
14. Lang F, Li X, Zheng W, *et al.*, 2017, CTCF Prevents Genomic Instability by Promoting Homologous Recombination-Directed DNA Double-Strand Break Repair. *Proc Natl Acad Sci U S A*, 114:10912–7.
DOI: 10.1073/pnas.1704076114
15. Canela A, Maman Y, Jung S, *et al.*, 2017, Genome Organization Drives Chromosome Fragility. *Cell*, 170:507–521.e518.
DOI: 10.1016/j.cell.2017.06.034
16. Hnisz D, Day DS, Young RA, 2016, Insulated Neighborhoods: Structural and Functional Units of Mammalian Gene Control. *Cell*, 167:1188–200.
DOI: 10.1016/j.cell.2016.10.024
17. Gibcus JH, Dekker J, 2013, The hierarchy of the 3D genome. *Mol Cell*, 49:773–82.
DOI: 10.1016/j.molcel.2013.02.011
18. Belton JM, McCord RP, Gibcus JH, *et al.*, 2012, Hi-C: A Comprehensive Technique to Capture the Conformation of Genomes. *Methods*, 58:268–76.
DOI: 10.1016/j.ymeth.2012.05.001
19. Li H, Durbin R, 2009, Fast and Accurate Short Read Alignment with Burrows-Wheeler Transform. *Bioinformatics*, 25:1754–60.
DOI: 10.1093/bioinformatics/btp324
20. Servant N, Varoquaux N, Lajoie BR, *et al.*, 2015, HiC-Pro: An Optimized and Flexible Pipeline for Hi-C Data Processing. *Genome Biol*, 16:259.
DOI: 10.1186/s13059-015-0831-x
21. Dixon JR, Gorkin DU, Ren B, 2016, Chromatin Domains: The Unit of Chromosome Organization. *Mol Cell*, 62:668–80.
DOI: 10.1016/j.molcel.2016.05.018
22. Guo Y, Xu Q, Canzio D, *et al.*, 2015, CRISPR Inversion of CTCF Sites Alters Genome Topology and Enhancer/Promoter Function. *Cell*, 162:900–10.
DOI: 10.1016/j.cell.2015.07.038
23. Lupiáñez DG, Spielmann M, Mundlos S, 2016, Breaking TADs: How Alterations of Chromatin Domains Result in Disease. *Trends Genet*, 32:225–37.
DOI: 10.1016/j.tig.2016.01.003
24. de Wit E, Vos ES, Holwerda SJ, *et al.*, 2015, CTCF Binding Polarity Determines Chromatin Looping. *Mol Cell*, 60:676–84.
DOI: 10.1016/j.molcel.2015.09.023
25. Narendra V, Rocha PP, An D, *et al.*, 2015, CTCF Establishes Discrete Functional Chromatin Domains at the Hox Clusters During Differentiation. *Science*, 347:1017–21.
DOI: 10.1126/science.1262088
26. Downen JM, Fan ZP, Hnisz D, *et al.*, 2014, Control of Cell Identity Genes Occurs in Insulated Neighborhoods in Mammalian Chromosomes. *Cell*, 159:374–87.
DOI: 10.1016/j.cell.2014.09.030
27. Reits EA, Hodge JW, Herberts CA, *et al.*, 2006, Radiation Modulates the Peptide Repertoire, Enhances MHC Class I Expression, and Induces Successful Antitumor Immunotherapy. *J Exp Med*, 203:1259–71.
DOI: 10.1084/jem.20052494
28. Weichselbaum RR, Liang H, Deng L, *et al.*, 2017, Radiotherapy and Immunotherapy: A Beneficial Liaison? *Nat Rev Clin Oncol*, 14:365–79.
DOI: 10.1038/nrclinonc.2016.211
29. Ray J, Munn PR, Vihervaara A, *et al.*, 2019, Chromatin Conformation Remains Stable Upon Extensive Transcriptional Changes Driven by Heat Shock. *Proc Natl Acad Sci U S A*, 116:19431–9.
DOI: 10.1073/pnas.1901244116
30. Li J, Liu Y, Duan P, *et al.*, 2018, NFκB Regulates HSF1 and cJun Activation in Heat Stress-Induced Intestinal Epithelial Cell Apoptosis. *Mol Med Rep*, 17:3388–96.
DOI: 10.3892/mmr.2017.8199

Publisher's note

Whioce Publishing remains neutral with regard to jurisdictional claims in published maps and institutional affiliations.